Eur. Phys. J. D (2018) 72: 83
https://doi.org/10.1140/epjd/e2017-80409-x

THE EUROPEAN PHYSICAL JOURNAL D

Regular Article

Magnetic field effects and waves in complex plasmas*

Hanno Kählert[1,a], André Melzer[2], Marian Puttscher[2], Torben Ott[1], and Michael Bonitz[1]

[1] Institut für Theoretische Physik und Astrophysik, Christian-Albrechts-Universität zu Kiel, Leibnizstr. 15, 24098 Kiel, Germany
[2] Institut für Physik, Ernst-Moritz-Arndt-Universität Greifswald, 17489 Greifswald, Germany

Received 14 June 2017
Published online 22 May 2018 – © EDP Sciences, Società Italiana di Fisica, Springer-Verlag 2018

Abstract. Magnetic fields can modify the physical properties of a complex plasma in various different ways. Weak magnetic fields in the mT range affect only the electrons while strong fields in the Tesla regime also magnetize the ions. In a rotating dusty plasma, the Coriolis force substitutes the Lorentz force and can be used to create an effective magnetization for the strongly coupled dust particles while leaving electrons and ions unaffected. Here, we present a summary of our recent experimental and theoretical work on magnetized complex plasmas. We discuss the dynamics of dust particles in magnetized discharges, the wave spectra of strongly coupled plasmas, and the excitations in confined plasmas.

1 Introduction

Complex (or dusty) plasmas usually contain small (micron-sized) dust particles, which are embedded in a partially ionized plasma of electrons, ions, and neutral gas particles [1]. Because of the apt spatial and temporal scales, the dynamics of individual dust particles can be recorded with video cameras allowing to retrieve the dust dynamics on the kinetic level. This has been a major reason why complex plasmas have emerged as an independent field of research for the study of strong correlations in plasmas [2,3]. The dust particles are highly susceptible to various forces in the plasma, such as electric fields or ion and neutral drag, and can serve as sensitive diagnostic tools. This applies to both single-particle measurements as well as the collective excitations of dust clouds [4–6].

The magnetization of a complex plasma is a topic of high current interest [7]. Due to the vastly different masses and charges of the three plasma components, the magnetization can be categorized into three stages. In the first stage, only the light electrons are magnetized. For the conditions of typical gas discharges, magnetic fields B of only a few mT are already sufficient. Although the ions are not magnetized, the averaged Hall component of the ion motion leads to a slow rotation of the dust cloud [8–12].

In the second stage, the heavy ions are magnetized as well. Due to their much higher mass, however, significantly stronger magnetic fields are required. Ion magnetization has been achieved using water-cooled [13] and superconducting magnets [14–16], which has led to a series of unexpected discoveries, including the filamentation of the entire discharge [15,17] or the formation of highly ordered dust structures when a grid electrode is used [16–18]. The interaction between two dust particles [19], which are aligned with the ion flow in the sheath region, and self-excited dust density waves [17] show a pronounced response to a strong external magnetic field. Also, self-excited vertical oscillations of the dust particles in a strongly magnetized plasma occur [20].

The third stage, where electrons, ions, and even the dust grains are magnetized, is the most challenging to reach. Based on different magnetization parameters, it was concluded [7] that small (nanometer-sized) dust particles would be required to magnetize the dust component along with the light species. A partial solution to this problem, based on a rotating setup, was presented in reference [21] and will be discussed in more detail below.

The magnetization of a plasma can be measured with several different parameters. Here, we focus on two particular choices. Effects of the magnetic field on the plasma species can, on the one hand, be described by the Hall parameter,

$$h_\alpha = \frac{\omega_{c\alpha}}{\nu_{\alpha n}}. \tag{1}$$

It relates the cyclotron frequency $\omega_{c\alpha} = q_\alpha B/m_\alpha$ of the species $\alpha = e, i, d$ (electrons, ions, dust) with charge q_α and mass m_α to their collision frequency $\nu_{\alpha n}$ with the neutral gas background of the plasma. A strong effect of the magnetic field can be expected when the particle motion is not significantly perturbed by collisions during a gyration period, i.e., when $h_\alpha > 1$.

* Contribution to the Topical Issue "Fundamentals of Complex Plasmas", edited by Jürgen Meichsner, Michael Bonitz, Holger Fehske, Alexander Piel.

[a] e-mail: kaehlert@theo-physik.uni-kiel.de

On the other hand, a magnetization parameter can be defined as the ratio of $\omega_{c\alpha}$ and the plasma frequency $\omega_{p\alpha} = [Dq_\alpha^2/(4\pi\epsilon_0 m_\alpha a_{ws,\alpha}^3)]^{1/2}$ (Wigner Seitz radius $a_{ws,\alpha}$, dimension D),

$$\beta_\alpha = \frac{\omega_{c\alpha}}{\omega_{p\alpha}}, \tag{2}$$

thus relating a fundamental frequency in the unmagnetized plasma with the cyclotron frequency. This parameter is particularly suited for the characterization of the collective modes in magnetized plasmas and has been employed frequently in studies of *strongly coupled plasmas*, see reference [22]. Here, it will be used only for the dust component.

The strong coupling regime is defined as the parameter region where the Coulomb coupling parameter [2],

$$\Gamma_\alpha = \frac{q_\alpha^2}{4\pi\epsilon_0 a_{ws,\alpha}} \frac{1}{k_B T_\alpha}, \tag{3}$$

is larger than unity, i.e., where the Coulomb interaction energy of two particles at a distance $a_{ws,\alpha}$ exceeds their kinetic energy, $k_B T_\alpha$. Here, T_α is the temperature of species α. In dusty plasmas, strong coupling effects occur as a consequence of the high charge on the dust particles, which can be on the order of several thousand elementary charges. The high charge can give rise to coupling strengths $\Gamma_d \gg 1$. Electrons and ions, on the other hand, remain weakly coupled with $\Gamma_{e,i} \ll 1$.

Even with the strongest magnetic fields available today, the direct magnetization of strongly coupled dust particles ($\beta_d > 1$) has not yet been achieved in a complex plasma experiment. An alternative approach has been proposed in references [21,22], where the inertial Coriolis force in a rotating reference frame serves as a substitute for the magnetic Lorentz force. While this approach leads to a strong "effective" magnetization of the dust particles, electrons and ions remain unmagnetized. Thus, even though a complete magnetization of a complex plasma cannot be achieved, a rotating dusty plasma allows one to study (pseudo) magnetization effects in a strongly coupled plasma for which simulations predict unusual properties due to the simultaneous effects of strong coupling and magnetization [23–25].

In the present work, we first give an overview over our recent experimental work on magnetized complex plasmas (Sect. 2), thereby covering mainly the magnetization of the light plasma components, i.e., electrons and ions. In these experiments, horizontal magnetic fields of up to 100 mT have been used as well as axial magnetic fields of up to 2 T in a particular experiment. In the second and third part, we focus on the collective modes of magnetized and confined strongly coupled plasmas. We first give an overview on the wave spectra of magnetized strongly coupled one-component plasmas and review recent experimental results for the waves in rotating dusty plasma under the influence of the Coriolis force (Sect. 3). In Section 4, we discuss a recent kinetic theory for the collective modes of strongly coupled plasmas in confinement potentials, which differ fundamentally from the waves in uniform plasmas. We conclude with a summary and an outlook on possible directions for future work in Section 5.

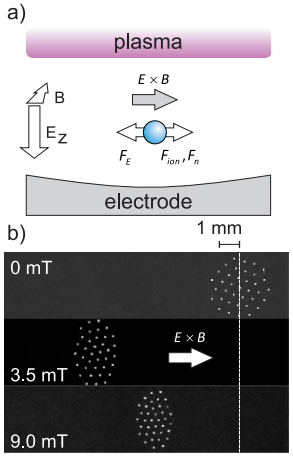

Fig. 1. (a) Sketch of the geometry. A horizontal magnetic field perpendicular to the sheath electric field is applied. The corresponding $\boldsymbol{E} \times \boldsymbol{B}$ direction and the direction of the various forces are indicated. (b) Top view of a dust cluster of 7.17 μm dust particles for different magnetic field strengths. It is seen that the cluster shows a complex sideways motion. After [26,27,29].

2 Influence of magnetic fields on complex plasmas

In a series of experiments [26–29], we have studied the influence of a horizontal magnetic field on the interaction of the dust with the plasma environment. There, the magnetic field has been oriented perpendicular to the sheath electric field E_z and, hence, a transverse $\boldsymbol{E} \times \boldsymbol{B}$ force arises. In an additional high-field experiment at Auburn University (MDPX) the influence of a strong, axial magnetic field on the dust is studied [20].

2.1 Transverse forces

One finds a quite complex reaction of the dust to a horizontal magnetic field and the evoked transverse forces (along or opposite to the $\boldsymbol{E} \times \boldsymbol{B}$ direction). As an example, a dust cluster of MF (melamine-formaldehyde) particles of 7.17 micrometer diameter is trapped in an argon rf-discharge at a gas pressure of 5 Pa. The entire cluster is vertically trapped by a force balance of electric field force and gravity, and horizontally confined by electrostatic forces due to a parabolic trough in the electrode. The behavior of the cluster is shown as a function of magnetic field strength in Figure 1b. First, at low magnetic fields the dust is forced to move in the confinement against the $\boldsymbol{E} \times \boldsymbol{B}$ (y-)direction. At larger fields, the particles move back along the $\boldsymbol{E} \times \boldsymbol{B}$ direction.

The sideways excursions y of dust particles of different size and at different gas pressure in the rf discharge are

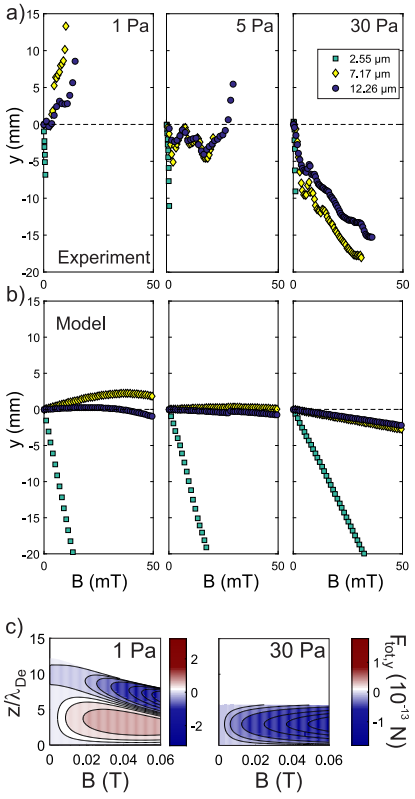

Fig. 2. (a) Measured sideways excursions y of dust particles of different size at a gas pressure of 1, 5 and 30 Pa. Positive values of y denote excursions in $\boldsymbol{E} \times \boldsymbol{B}$ direction. (b) Sideways excursions for the experimental situation derived from a model of the magnetized sheath and the corresponding forces acting on the dust. (c) Net force in the sheath as a function of vertical position in the sheath z and magnetic field strength. Positive values of $F_{\mathrm{tot},y}$ indicate a force in $\boldsymbol{E} \times \boldsymbol{B}$ direction. After [27,29].

given in Figure 2a. Depending on the parameters, the particles either move along $\boldsymbol{E} \times \boldsymbol{B}$ or opposite to it or even perform a more complex motion.

Qualitatively, the electrons are immediately magnetized (already $h_{\mathrm{e}} = 2.5$ at $B = 1\,\mathrm{mT}$ and $p = 5\,\mathrm{Pa}$) and thus follow the $\boldsymbol{E} \times \boldsymbol{B}$ drift. The ions are unmagnetized ($h_{\mathrm{i}} < 1$ up to $B = 140\,\mathrm{mT}$ at $p = 5\,\mathrm{Pa}$) and thus are nearly unaffected by the magnetic field. Due to this charge separation a horizontal ambipolar electric field in $\boldsymbol{E} \times \boldsymbol{B}$ direction between electrons and ions arises [30,31]. Now, this ambipolar electric field establishes an ion flow and thus an ion drag force on the dust that drives the dust in the $\boldsymbol{E} \times \boldsymbol{B}$ direction. Moreover, at higher gas pressure, also the momentum transfer of the ions to the neutral argon atoms becomes more and more important. The neutral atoms are set into motion in ion direction and can drive the dust via the neutral drag force [11], again in the $\boldsymbol{E} \times \boldsymbol{B}$ direction. Due to the negative dust charge, the electric field force on the dust is opposed to $\boldsymbol{E} \times \boldsymbol{B}$ [27], see also Figure 1a. It is now a question of the delicate force balance between the ion and neutral drag on the one hand and the electric force on the other hand that determines in which direction the dust is moved.

A quantitative understanding can be gained by solving models of the magnetized sheath [32–34]. From the model, the transverse ion flow velocity $u_{\mathrm{i}y}$ in the $\boldsymbol{E} \times \boldsymbol{B}$ direction is derived for the specific parameters of the experiment, see Figure 2b. This transverse ion velocity directly determines the ion drag force and, via collisions with the neutral gas, the neutral drag force. In addition, since the ion flow is coupled to the ambipolar electric field via the ion mobility, also the opposing electric field force is derived (one could in principle also account for the Hall component of the ion flow, but that is usually not necessary since in most cases $h_i < 1$). With that the force balance on the dust has been analyzed for the magnetized sheath [29].

From the solution of the model for the entire sheath (here, z denotes the vertical position from the sheath edge at $z = 0$ to the electrode), it is seen that the forces on the dust is against $\boldsymbol{E} \times \boldsymbol{B}$ throughout the sheath at higher gas pressures (Fig. 2c) , in agreement to what is observed in the experiment. At lower gas pressures, the situation is more complicated. Near the sheath edge, where the transverse ion flow velocity is small, the ion drag exceeds the electric field force [29]. This is similar to the situation for the formation of the central dust-free void in such rf discharges [35–37]. There, in the plasma center, the ion flow due to ambipolar electric fields is small (due to symmetry), but nevertheless the ion drag exceeds the electric field force and is thus responsible for the formation of the void. Here, in the sheath, again the ion drag force dominates for low ion velocities. Deeper in the sheath, however, the electric field force due to stronger ambipolar fields is larger than the ion drag. Hence, the horizontal motion of the dust in the sheath is also coupled to its vertical equilibrium position.

2.2 Vertical interaction in the sheath

Besides the horizontal force balance, also the vertical interaction of a dust particle in the plasma sheath environment is modified by magnetic fields.

A dust particle trapped in the sheath influences another particle lower in the sheath by a non-reciprocal attractive wakefield [38–42]. The wakefield is a region of enhanced positive ion space-charge that is formed below a dust particle by the ion streaming motion through the sheath past the dust particle. This wakefield interaction is affected by a magnetic field [19,43,44]. In an experimental situation as described previously with a horizontal magnetic field, at low magnetic field strength two dust particles are found vertically aligned due to the wakefield interaction, see Figure 3a. With increasing magnetic field the ensemble moves sideways as described above. However, at a certain magnetic field strength the vertical alignment is broken. Two different reasons have been identified for this: first, due to their different levitation height the two dust particles experience different transverse forces that drive the break-up of the alignment. Second, direct laser manipulation of the dust particle pair reveals that also the wakefield is weakened by the magnetic field [28].

In a completely different experiment with a strong axial (vertical) magnetic field of up to more than 2 T, one

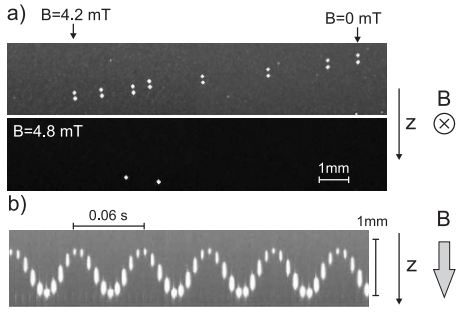

Fig. 3. (a) Overlay of several video frames showing the sideways motion of a pair of dust particles in the sheath due to a horizontal magnetic field from 0 to 4.2 mT. At about 4.8 mT the alignment is broken and the particles become separated. (b) Composed spatio-temporal image showing the vertical oscillations of a dust particle under a strong axial magnetic field of $B = 2.27$ T. After [20,28].

finds that the magnetic field strongly influences the dust particle structure by imposing the grid pattern of the electrode onto the dust particle arrangement [16] or by modifying the wakefield interaction [19]. In such an experiment (MDPX at Auburn University, with grid electrode), we have observed self-excited vertical oscillations of dust particles trapped in the sheath [20], see Figure 3b. The vertical oscillations can be triggered by illuminating the dust with a low-power laser. The self-oscillatory behavior can be explained by a delayed-charging mechanism [45,46] where the instantaneous charge on a dust particle during the oscillation path is different from its equilibrium charge at that point. This occurs when the particle travels through a region with a charge gradient under finite charging times, so that on the one way it has a charge higher than the equilibrium and on the return path a charge that is lower than the equilibrium charge. Magnetic fields seem to favor the formation of a charge gradient in the sheath due to the fact that the electron gyro-radius is of the order of the dust size at these magnetic field strengths and the electron mobility transverse to the field is hindered. A charge gradient that is compatible with the observations would be of the order of 1×10^3 elementary charges per mm (with the lower charge number at the upper point of the trajectory) [20]. It should be noted, that even under the conditions of this high magnetic field the Hall parameter for the dust h_d can be estimated to be of the order of 10^{-4}, so direct magnetization effects of the dust can be excluded.

3 Waves in magnetized strongly coupled (dusty) plasmas

In this section, we consider the wave spectra of strongly coupled magnetized plasmas. We first discuss the predictions of theoretical approaches and molecular dynamics simulations for the waves in one-component plasmas and then discuss recent experimental results for the wave spectrum of a rotating two-dimensional dusty plasma.

3.1 Theoretical predictions for the wave spectra

The Yukawa One-Component Plasma [47], where the particles interact via a screened Coulomb (Yukawa) potential, $v(r) = q_d^2 \exp(-r/\lambda)/(4\pi\epsilon_0 r)$ (screening length λ), often serves as a simple yet sufficiently accurate model to describe the waves in *two-dimensional* dust layers. Simulations and theoretical calculations show that both the longitudinal mode and the transverse shear mode, the latter of which exists only due to strong coupling effects, acquire a mixed polarization in a magnetic field [48,49]. In addition, a frequency gap between the two modes is formed, which increases with the magnetization. Interestingly, strong magnetization leads to the emergence of higher harmonics of the so-called magnetoplasmon at high wavenumbers [50]. Their properties and existence conditions in dusty plasmas have been investigated in detail with simulations [49].

The most fundamental theoretical model for a *three-dimensional* strongly coupled plasma is the One-Component plasma (OCP): N charged particles embedded in a uniform background of the opposite charge. Based on the Quasilocalized Charge Approximation (QLCA) [51] and molecular dynamics simulations, a comprehensive analysis of its collective modes has been presented in reference [52]. As an external magnetic field $\boldsymbol{B}$ breaks the isotropy of the plasma, wave propagation depends on the orientation between the wave vector $\boldsymbol{k}$ and the magnetic field direction. Along the field direction, magnetization lifts the degeneracy of the two transverse shear modes and leads to the formation of an upper and a lower shear mode. In the perpendicular direction, on the other hand, the emergence of two hybrid modes with unusual polarization properties has been reported, akin to those in 2D (see above). Moreover, similar to the observations in two-dimensional Yukawa systems, a strong magnetic field gives rise to higher harmonics due to the successive nonlinear interaction of the fundamental modes [52].

While wave propagation under oblique angles has been investigated using the QLCA in reference [53], additional molecular dynamics simulation results and a comparison with angle-averaged harmonic lattice theory (AAHL) and the QLCA have been presented in reference [54]. A direct comparison between simulations, AAHL, and the QLCA is shown in Figure 4 for a coupling parameter $\Gamma = 150$, i.e., deep in the strongly coupled regime. While the theoretical models yield very similar results for the high-frequency modes (upper hybrid and upper shear mode, plasmon), AAHL is in better agreement with the simulation data for the low-frequency modes (lower hybrid and lower shear mode, ordinary shear mode). However, at lower coupling, the QLCA gains an advantage and compares more favorably with the simulations [54].

3.2 Pseudo-magnetization of a dusty plasma

The magnetization of the strongly coupled dust particles in a complex plasma has, so far, not been achieved by ordinary means, i.e., via a strong magnetic field. The reason is the high mass of the dust particles, which would require

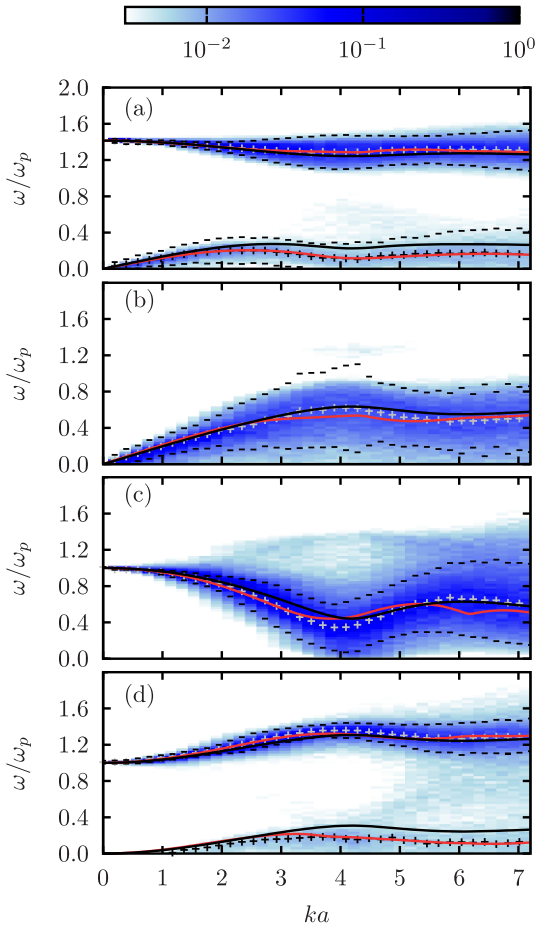

Fig. 4. Comparison of molecular dynamics simulations (color scale; gray and black symbols denote peak positions and widths, respectively), AAHL (red lines), and the QLCA (black lines) for the three-dimensional One-Component plasma at $\Gamma = 150$ with $\beta = 1$. (a) Upper and lower hybrid modes ($\boldsymbol{k} \perp \boldsymbol{B}$), (b) ordinary shear mode ($\boldsymbol{k} \perp \boldsymbol{B}$), (c) plasmon ($\boldsymbol{k}||\boldsymbol{B}$), (d) upper and lower shear modes ($\boldsymbol{k}||\boldsymbol{B}$). Adapted from [54]. Copyright (2013) by the American Physical Society.

enormous magnetic field strengths (on the order of 10^3–10^4 T [21]) to increase the magnetization parameter [see Eq. (2)],

$$\beta_\mathrm{d} = \frac{\omega_\mathrm{cd}}{\omega_\mathrm{pd}} \propto \frac{B}{\sqrt{m_\mathrm{d}}}, \tag{4}$$

to values $\beta_\mathrm{d} \sim 1$.

The approach of reference [21] avoids the unfavorable scaling relation by resorting to the Coriolis force, $\boldsymbol{F}_\mathrm{c} = 2m\boldsymbol{v}' \times \boldsymbol{\Omega}$, acting on a dust particle with velocity $\boldsymbol{v}'$ in a coordinate system rotating with angular velocity $\boldsymbol{\Omega} = \Omega\hat{\boldsymbol{e}}_\Omega$. Its mathematical structure is fully equivalent to the Lorentz force, $\boldsymbol{F}_\mathrm{L} = Q\boldsymbol{v} \times \boldsymbol{B}$, but the scaling with the dust mass and the dust charge is completely different. In particular, the effective cyclotron frequency is given by $\omega_\mathrm{c}^\mathrm{eff} = 2\Omega$, i.e., it is independent of the charge and the mass. Typical experimental rotation frequencies of several Hz are comparable to the dust plasma frequency but the natural timescales for electrons and ions are much shorter. As a result, electrons and ions are not affected by the slow rotation but the dust particles can be strongly "magnetized".

In experiments, the rotation of the dust particles is induced via the neutral drag force exerted on the particles by a rotating neutral gas column [11]. The potential of the method was demonstrated in a proof-of-principle experiment, where the normal modes of a small cluster with four particles were determined [21]. The results for the mode frequencies were in excellent agreement with theoretical calculations, which also accounted for the centrifugal force in the rotating frame, which leads to a weaker confinement of the dust particles and limits the rotation frequencies to values below a critical limit [21].

The approach was later extended to two-dimensional dust layers [22,55]. Theoretical estimations based on a harmonic confinement potential for the dust particles indicated that $\beta_\mathrm{d} \sim 1$ could be achieved, but the centrifugal force might be a limiting factor [22]. In the "RotoDust" setup of reference [55], an additional glass cylinder was placed on the lower electrode to create a stronger confinement for the dust and to balance the centrifugal force at high rotation rates. Instead of the normal modes of a small cluster, as in reference [21], the longitudinal wave spectra of two-dimensional layers with several hundred particles were analyzed.

The results of the experiment have been compared with molecular dynamics simulations [55], see Figure 5. In the long-wavelength limit, the experiments show a pronounced excitation close to the effective cyclotron frequency $\omega_\mathrm{c}^\mathrm{eff} = 2\Omega$, as predicted by theory and simulation [48–50]. For finite wavenumbers, the wave frequency increases until the excitation eventually disappears at large k. The molecular dynamics simulations show a very similar behavior for the dispersion relation. A more detailed comparison shows that the peak positions of experiment and simulation closely agree in all three cases, see reference [55].

4 Collective modes of strongly coupled confined complex plasmas

Dust clusters with small particle numbers often exhibit finite-size effects, which affect their structural properties as well as their collective modes. Yukawa balls, for example, are spherical dust clouds with a well-defined shell structure under strong coupling conditions [56]. The formation of the shells and their occupation numbers can be explained theoretically with a model based on an isotropic harmonic confinement, which summarizes the various plasma forces acting on the dust particles [57]. The collective modes of Yukawa balls [58–61] and other confined plasmas (ions in traps [62], ultracold neutral plasmas [63]) are affected by surface effects as well, and thus strongly differ from the waves in an extended uniform plasma.

A challenge for theory is to include strong coupling and confinement effects at the same time. A kinetic theory for confined strongly coupled plasmas has been proposed in

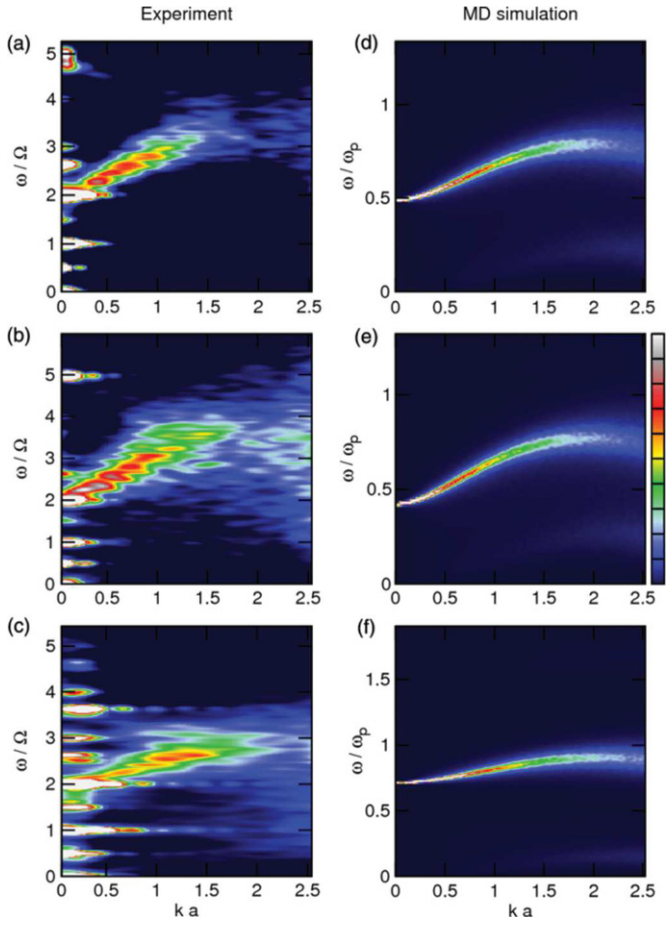

Fig. 5. Longitudinal current fluctuation spectra obtained from the "RotoDust" experiment (left) compared with molecular dynamics simulations for a magnetized two-dimensional Yukawa plasma (coupling parameter $\Gamma_\mathrm{d} = 120$) (right). The frequency axis for the experimental data is scaled to the rotation frequency Ω. The corresponding (effective) magnetization parameters entering the simulations are (d) $\beta_\mathrm{d} = 0.52$, (e) $\beta_\mathrm{d} = 0.45$, and (f) $\beta_\mathrm{d} = 0.76$. From [55]. Copyright (2013) by the American Physical Society.

reference [64]. It is based on an extension of the Singwi-Tosi-Land-Sjölander (STLS) ansatz for the two-particle distribution function [65]. Instead of using the static equilibrium pair distribution function to include correlation effects in the two-particle distribution function $f^{(2)}$, the pair correlations are made time-dependent by writing $f^{(2)}$ as

$$f^{(2)}(\boldsymbol{r}_1, \boldsymbol{p}_1, \boldsymbol{r}_2, \boldsymbol{p}_2, t) = f(\boldsymbol{r}_1, \boldsymbol{p}_1, t) f(\boldsymbol{r}_2, \boldsymbol{p}_2, t) g(\boldsymbol{r}_1, \boldsymbol{r}_2, t). \quad (5)$$

Here, $f(\boldsymbol{r}, \boldsymbol{p}, t)$ is the one-particle distribution function and $g(\boldsymbol{r}_1, \boldsymbol{r}_2, t)$ the time-dependent pair distribution. The positions and momenta of the particle with index i are denoted by $\boldsymbol{r}_i$ and $\boldsymbol{p}_i$, respectively.

Equation (5) and the original STLS ansatz simplify the description of the correlations by assuming that the pair distribution function does not depend on the momenta.

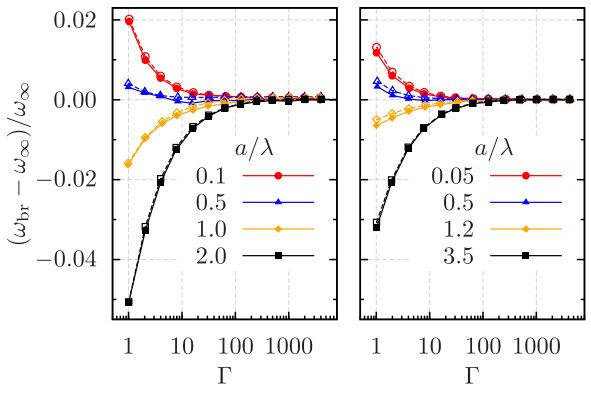

Fig. 6. Comparison between the predictions of the extended STLS theory (dashed lines, open symbols) and molecular dynamics simulations (solid lines, full symbols) for the breathing mode frequency of confined Yukawa clusters with 200 particles in three dimensions (left) and two dimensions (right). From [64]. Copyright (2014) by the American Physical Society.

The time evolution of g in the extended STLS scheme of reference [64] was determined from the second equation of the BBGKY hierarchy, which leads to

$$\frac{\partial g}{\partial t} + \nabla_{\boldsymbol{r}_1} g \cdot \boldsymbol{u}(\boldsymbol{r}_1, t) + \nabla_{\boldsymbol{r}_2} g \cdot \boldsymbol{u}(\boldsymbol{r}_2, t) = 0. \quad (6)$$

Here, $\boldsymbol{u}(\boldsymbol{r}, t)$ is the fluid velocity field. The dynamical equation for f is formally identical to the Vlasov equation but includes an additional correlation force, which is calculated from the correlation function and the particle density.

The theory has been applied to the breathing oscillations of two- and three-dimensional dust clusters in a harmonic confinement, $V(r) = m_\mathrm{d}\omega_0^2 r^2/2$, where ω_0 is the trap frequency [64]. The breathing mode [66,67] is a purely radial excitation and can be excited selectively with laser light in experiments with two-dimensional dust clusters [68]. In order to determine its frequency, the kinetic equation of reference [64] has been used to derive simpler fluid equations, from which the breathing frequency could be deduced. A direct comparison between molecular dynamics simulations and the theoretical results is shown in Figure 6 as a function of the coupling strength $\Gamma = q_\mathrm{d}^2/(4\pi\epsilon_0 a)$, where the Wigner–Seitz radius in equation (3) has been replaced by $a = [q_\mathrm{d}^2/(4\pi\epsilon_0 m_\mathrm{d}\omega_0^2)]^{1/3}$. The theory is in very good agreement with the simulations for all coupling strengths, screening parameters a/λ, and for two- and three-dimensional systems [64].

In order to provide a simplified description of correlations in inhomogeneous plasmas, a reduced theory for the collective modes has been derived from the fluid equations [69]. The reduced description incorporates strong coupling effects via space-dependent bulk and shear moduli, which are calculated from the pair correlation function of an associated uniform system with the local particle density. This is in contrast to the fluid theory of reference [64], which is fully nonlocal and includes the complete (inhomogeneous) pair correlation function of the plasma. The resulting equations in the reduced model are considerably

less complex but can only be applied when the spatial variations of the density are sufficiently weak or low-order modes are considered.

5 Conclusions

In summary, we have covered several aspects of complex plasmas under magnetic fields characterized by a wide range of Hall parameters h_α and magnetization parameters β_α.

In experiments under low magnetic fields ($h_e > 1$ but $h_i \leq 1$), the motion of dust particles trapped in the sheath is affected by transverse forces along or opposite to $\boldsymbol{E} \times \boldsymbol{B}$ direction [26,27]. The reason is a transverse ion flow that excites ion and neutral drag forces on the one hand and electric field forces on the other hand. The delicate force balance between these forces determines the dust particle motion. The forces can be derived quantitatively from models of the magnetized sheath [29,32,33]. In addition, also the wakefield interaction between vertically aligned particle pairs in the sheath is modified by these transverse forces [28].

In stronger, axial fields, where $h_e \gg 1$ and $h_i > 1$, self-excited vertical oscillations appear that might be explained by delayed-charging effects due to the strongly modified charging dynamics of the dust in the sheath [20].

Two independently performed experiments [21,55] show that it is possible to mimic the behavior of a strongly coupled plasma with a confined dust cloud that corotates with a neutral gas column. In particular, the experiments have confirmed the predicted change of the excitation spectra when the plasma becomes (pseudo) magnetized. Future experiments could investigate the freezing transition [70] or address the hydrodynamic properties of magnetized strongly coupled plasmas [24,25,71]. In particular, the combined influence of strong coupling and strong magnetization on the viscosity coefficients is largely unknown, which are highly important for an accurate description of momentum transport and the collective modes.

This work is supported by the DFG via SFB-TR24, projects A3, A5 and A7, and by a grant for CPU time at the HLRN. We thank H. Löwen (Düsseldorf), G.J. Kalman (Boston), Z. Donkó (Budapest), P. Hartmann (Budapest), and D.A. Baiko (St. Petersburg) for their contributions to many of the results cited and for interesting and stimulating discussions over the recent years.

Author contribution statement

A.M. and M.P. conceived and evaluated the described experiments in Section 2, the experiments were prepared and performed by M.P. The molecular dynamics simulations for magnetized macroscopic (confined) plasmas were performed by T.O. (H.K.). The theoretical results were worked out by H.K., T.O., and M.B.
All the authors were involved in the preparation of the manuscript. All the authors have read and approved the final manuscript.

References

1. P.K. Shukla, B. Eliasson, Rev. Mod. Phys. **81**, 25 (2009)
2. M. Bonitz, C. Henning, D. Block, Rep. Prog. Phys. **73**, 066501 (2010)
3. G.E. Morfill, A.V. Ivlev, H.M. Thomas, Phys. Plasmas **19**, 055402 (2012)
4. P.K. Shukla, A.A. Mamun, *Introduction to dusty plasma physics* (Institute of Physics Publishing, Bristol, 2002)
5. A. Piel, *Plasma physics: an introduction to laboratory, space, and fusion plasmas* (Springer, Heidelberg, 2010)
6. V.E. Fortov, A.V. Ivlev, S.A. Khrapak, A.G. Khrapak, G.E. Morfill, Phys. Rep. **421**, 1 (2005)
7. E. Thomas Jr., R.L. Merlino, M. Rosenberg, Plasma Phys. Control. Fusion **54**, 124034 (2012)
8. U. Konopka, D. Samsonov, A.V. Ivlev, J. Goree, V. Steinberg, G.E. Morfill, Phys. Rev. E **61**, 1890 (2000)
9. F. Cheung, A. Samarian, B. James, New J. Phys. **5**, 75 (2003)
10. V.Y. Karasev, E.S. Dzlieva, A.Y. Ivanov, A.I. Eikhvald, Phys. Rev. E **74**, 066403 (2006)
11. J. Carstensen, F. Greiner, L.J. Hou, H. Maurer, A. Piel, Phys. Plasmas **16**, 013702 (2009)
12. T. Reichstein, J. Wilms, F. Greiner, A. Piel, A. Melzer, Contrib. Plasma Phys. **52**, 813 (2012)
13. B. Tadsen, F. Greiner, A. Piel, Phys. Plasmas **21**, 103704 (2014)
14. N. Sato, G. Uchida, T. Kaneko, S. Shimizu, S. Iizuka, Phys. Plasmas **8**, 1786 (2001)
15. M. Schwabe, U. Konopka, P. Bandyopadhyay, G.E. Morfill, Phys. Rev. Lett. **106**, 215004 (2011)
16. E. Thomas Jr., B. Lynch, U. Konopka, R.L. Merlino, M. Rosenberg, Phys. Plasmas **22**, 030701 (2015)
17. E. Thomas Jr., U. Konopka, R.L. Merlino, M. Rosenberg, Phys. Plasmas **23**, 055701 (2016)
18. E. Thomas Jr., U. Konopka, B. Lynch, S. Adams, S. LeBlanc, R.L. Merlino, M. Rosenberg, Phys. Plasmas **22**, 113708 (2015)
19. J. Carstensen, F. Greiner, A. Piel, Phys. Rev. Lett. **109**, 135001 (2012)
20. M. Puttscher, A. Melzer, U. Konopka, S. LeBlanc, B. Lynch, E. Thomas Jr., Phys. Plasmas **24**, 013701 (2017)
21. H. Kählert, J. Carstensen, M. Bonitz, H. Löwen, F. Greiner, A. Piel, Phys. Rev. Lett. **109**, 155003 (2012)
22. M. Bonitz, H. Kählert, T. Ott, H. Löwen, Plasma Sources Sci. Technol. **22**, 015007 (2013)
23. T. Ott, M. Bonitz, Phys. Rev. Lett. **107**, 135003 (2011)
24. T. Ott, H. Löwen, M. Bonitz, Phys. Rev. E **89**, 013105 (2014)
25. T. Ott, M. Bonitz, Z. Donkó, Phys. Rev. E **92**, 063105 (2015)
26. M. Puttscher, A. Melzer, New J. Phys. **16**, 043026 (2014)
27. M. Puttscher, A. Melzer, Phys. Plasmas **21**, 123704 (2014)
28. M. Puttscher, A. Melzer, Phys. Plasmas **22**, 073701 (2015)
29. A. Melzer, M. Puttscher, Phys. Plasmas **24**, 053701 (2017)
30. S.C. Yang, Y. Nakajima, Y. Maemura, Y. Matsuda, H. Fujiyama, Plasma Sources Sci. Technol. **5**, 333 (1996)
31. Y. Maemura, S.C. Yang, H. Fujiyama, Surf. Coat. Technol. **98**, 1351 (1998)
32. B.P. Pandey, S.V. Vladimirov, A. Samarian, Phys. Plasmas **18**, 053703 (2011)
33. H. Mehdipour, I. Denysenko, K. Ostrikov, Phys. Plasmas **17**, 123708 (2010)

34. G. Foroutan, H. Mehdipour, H. Zahed, Phys. Plasmas **16**, 103703 (2009)
35. J. Goree, G. Morfill, V. Tsytovich, S.V. Vladimirov, Phys. Rev. E **59**, 7055 (1999)
36. M. Akdim, W. Goedheer, Phys. Rev. E **65**, 015401 (2001)
37. M. Kretschmer, S.A. Khrapak, S.K. Zhdanov, H.M. Thomas, G.E. Morfill, V.E. Fortov, A.M. Lipaev, V.I. Molotkov, A.I. Ivanov, M.V. Turin, Phys. Rev. E **71**, 056401 (2005)
38. S.V. Vladimirov, M. Nambu, Phys. Rev. E **52**, R2172 (1995)
39. M. Nambu, S.V. Vladimirov, P.K. Shukla, Phys. Lett. A **203**, 40 (1995)
40. V.A. Schweigert, I.V. Schweigert, A. Melzer, A. Homann, A. Piel, Phys. Rev. E **54**, 4155 (1996)
41. A. Melzer, V.A. Schweigert, I.V. Schweigert, A. Homann, S. Peters, A. Piel, Phys. Rev. E **54**, R46 (1996)
42. H. Jung, F. Greiner, O.H. Asnaz, J. Carstensen, A. Piel, Phys. Plasmas **22**, 053702 (2015)
43. J.P. Joost, P. Ludwig, H. Kählert, C. Arran, M. Bonitz, Plasma Phys. Control. Fusion **57**, 025004 (2015)
44. P. Ludwig et al., Eur. Phys. J. D **72**, 82 (2018)
45. S. Nunomura, T. Misawa, N. Ohno, S. Takamura, Phys. Rev. Lett. **83**, 1970 (1999)
46. A. Ivlev, U. Konopka, G. Morfill, Phys. Rev. E **62**, 2739 (2000)
47. Z. Donkó, G.J. Kalman, P. Hartmann, J. Phys.: Condens. Matter **20**, 413101 (2008)
48. L.J. Hou, P.K. Shukla, A. Piel, Z.L. Mišković, Phys. Plasmas **16**, 073704 (2009)
49. T. Ott, M. Bonitz, P. Hartmann, Z. Donkó, Phys. Rev. E **83**, 046403 (2011)
50. M. Bonitz, Z. Donkó, T. Ott, H. Kählert, P. Hartmann, Phys. Rev. Lett. **105**, 055002 (2010)
51. K.I. Golden, G.J. Kalman, Phys. Plasmas **7**, 14 (2000)
52. T. Ott, H. Kählert, A. Reynolds, M. Bonitz, Phys. Rev. Lett. **108**, 255002 (2012)
53. H. Kählert, T. Ott, A. Reynolds, G.J. Kalman, M. Bonitz, Phys. Plasmas **20**, 057301 (2013)
54. T. Ott, D.A. Baiko, H. Kählert, M. Bonitz, Phys. Rev. E **87**, 043102 (2013)
55. P. Hartmann, Z. Donkó, T. Ott, H. Kählert, M. Bonitz, Phys. Rev. Lett. **111**, 155002 (2013)
56. O. Arp, D. Block, A. Piel, A. Melzer, Phys. Rev. Lett. **93**, 165004 (2004)
57. M. Bonitz, D. Block, O. Arp, V. Golubnychiy, H. Baumgartner, P. Ludwig, A. Piel, A. Filinov, Phys. Rev. Lett. **96**, 075001 (2006)
58. H. Kählert, M. Bonitz, Phys. Rev. E **82**, 036407 (2010)
59. H. Kählert, M. Bonitz, Phys. Rev. E **83**, 056401 (2011)
60. A. Schella, M. Mulsow, A. Melzer, H. Kählert, D. Block, P. Ludwig, M. Bonitz, New J. Phys. **15**, 113021 (2013)
61. A. Piel, Plasma Phys. Control. Fusion **59**, 014001 (2017)
62. A. Dantan, J.P. Marler, M. Albert, D. Guénot, M. Drewsen, Phys. Rev. Lett. **105**, 103001 (2010)
63. A. Lyubonko, T. Pohl, J.M. Rost, New J. Phys. **14**, 053039 (2012)
64. H. Kählert, G.J. Kalman, M. Bonitz, Phys. Rev. E **90**, 011101(R) (2014)
65. K.S. Singwi, M.P. Tosi, R.H. Land, A. Sjölander, Phys. Rev. **176**, 589 (1968)
66. C. Henning, K. Fujioka, P. Ludwig, A. Piel, A. Melzer, M. Bonitz, Phys. Rev. Lett. **101**, 045002 (2008)
67. A. Olivetti, J. Barré, B. Marcos, F. Bouchet, R. Kaiser, Phys. Rev. Lett. **103**, 224301 (2009)
68. J. Schablinski, D. Block, Phys. Plasmas **22**, 023703 (2015)
69. H. Kählert, G.J. Kalman, M. Bonitz, Contrib. Plasma Phys. **55**, 352 (2015)
70. T. Ott, H. Löwen, M. Bonitz, Phys. Rev. Lett. **111**, 065001 (2013)
71. T. Ott et al., Eur. Phys. J. D **72**, 84 (2018)